

Propagation properties of Airy–Gaussian vortex beams through the gradient-index medium

RUIHUANG ZHAO,^{1,2} FU DENG,^{1,2} WEIHAO YU,^{1,2} JIAYAO HUANG,^{1,2} AND DONGMEI DENG^{1,2,*}

¹Guangdong Provincial Key Laboratory of Nanophotonic Functional Materials and Devices, South China Normal University, Guangzhou 510631, China

²CAS Key Laboratory of Geospace Environment, University of Sciences Technology of China, Chinese Academy of Sciences, Hefei 230026, China

*Corresponding author: dmdeng@263.net

Received 24 February 2016; revised 13 April 2016; accepted 13 April 2016; posted 13 April 2016 (Doc. ID 259811); published 9 May 2016

Propagation of Airy–Gaussian vortex (AiGV) beams through the gradient-index medium is investigated analytically and numerically with the transfer matrix method. Deriving the analytic expression of the AiGV beams based on the Huygens diffraction integral formula, we obtain the propagate path, intensity and phase distributions, and the Poynting vector of the first- and second-order AiGV beams, which propagate through the paraxial *ABCD* system. The ballistic trajectory is no longer conventional parabolic but trigonometric shapes in the gradient-index medium. Especially, the AiGV beams represent the singular behavior at the propagation path and the light intensity distribution. The phase distribution and the Poynting vector exhibit in reverse when the AiGV beams through the singularity. As the order increases, the main lobe of the AiGV beams is gradually overlapped by the vortex core. Further, the sidelobe weakens when the AiGV beams propagate nearly to the singularity. Additionally, the figure of the Poynting vector of the AiGV beams proves the direction of energy flow corresponding to the intensity distribution. The vortex of the second-order AiGV beams is larger, and the propagation velocity is faster than that of the first order. © 2016 Optical Society of America

OCIS codes: (010.3310) Laser beam transmission; (050.4865) Optical vortices; (050.5080) Phase shift; (070.2580) Paraxial wave optics; (070.2590) ABCD transforms; (310.3840) Materials and process characterization.

<http://dx.doi.org/10.1364/JOSAA.33.001025>

1. INTRODUCTION

Nondiffracting is part of the optical wave packet that keeps its own optical property in free-space transmission. The Airy beam, which is a new kind of nondiffracting beam, can be generated by a Gaussian beam through the cubic phase modulation and Fourier transform lens [1–3]. The property of the Airy beam is self-healing in the propagation process and has the characteristics of lateral acceleration, which is similar to ballistic movement under action of gravity [4]. Baumgartl and coworkers [5] used the Airy wave packet to clean the optical particle in the local zone. It makes the Airy beam blow the particle to the main sidelobe, driven by the energy flux. Because of its unique properties, the Airy beam has attracted widespread attention [3–8].

On the other hand, the Airy–Gaussian (AiG) beams, from which the Airy beam carries finite energy, have nondiffracting propagation properties within a finite distance. Nowadays, the AiG beams have been studied based on its theoretical and experimental research. The AiG beams show a self-healing nature and parabolic trajectory propagating on the free space and the uniaxial crystal. What is more, based on the AiG beams, the

Airy–Gaussian vortex (AiGV) beams are multiplied by a vortex factor. The vortex beam, which owns continuous spiral phase, has phase singularity and intensity singularity [9]. Because of the vortex factor, the main lobe or the sidelobe of the AiG beams will be destroyed, depending on the direction of vortex. Owing to the influence of vortex, the nondiffracting of the AiGV beams can be shown after propagating at a distance. As a new type of nondiffracting beam, the AiGV beams have to be further researched propagating in the gradient-index medium to perform some special properties. The gradient-index medium has application value in photocommunication, techniques of optical sensing, and fiber splicing. The lateral variation of the refractive index also makes the light beam generate in a lens-like and waveguide effect, so that the propagation effects of AiG beams are different from others [10]. There has been research on the fully spatially coherent light and the partially coherent polychromatic light propagating in the gradient-index medium [10–12].

Based on the generalized Huygens–Fresnel integral formula, the passage derived analytical propagation expressions in regards to the AiGV beams, which propagate in the paraxial

$ABCD$ system. Using numerical simulations, we discover that the ballistic trajectory and the track of the vortex of the first- and second-order AiGV beams exist singularity through the gradient-index medium. We also study the intensity and phase distribution of the AiGV beams in the gradient-index medium. Further, we investigate the influence of different Z_0 values on the propagation of the first- and second-order AiGV beams through the gradient-index medium. Besides, we analyze that the effect of the vortex to the Poynting vector of the first- and second-order AiGV beams.

2. ANALYTICAL EXPRESSION OF THE FIRST- AND SECOND-ORDER AIGV BEAMS THROUGH THE GRADIENT-INDEX MEDIA

In the initial plane, the field distribution of the AiGV beams superimposed by an order can be expressed as [1,13]

$$E_0(x_0, y_0, 0) = A_0 \text{Ai} \left(\frac{x_0}{w_1} \right) \text{Ai} \left(\frac{y_0}{w_2} \right) \exp \left(\frac{a_1 x_0}{w_1} + \frac{a_2 y_0}{w_2} \right) \times \exp \left(-\frac{x_0^2 + y_0^2}{w_0^2} \right) \left(\frac{x_0 - x_d}{w_1} + i \frac{y_0 - y_d}{w_2} \right)^l, \quad (1)$$

where $E_0(x_0, y_0, 0)$ represents the initial electric field distribution at the input plane, A_0 denotes the constant amplitude, and $\text{Ai}(\cdot)$ is the Airy function [14], w_0 is the arbitrary transverse scales and $0 \leq a_1 < 1$, $0 \leq a_2 < 1$ in the exponential function is a parameter associated with the truncation of the AiGV beams, w_1 and w_2 are arbitrary transverse scales in x and y directions, respectively, among of which, w_1 can be expressed as $w_1 = \chi_0 w_0$ and $w_2 = \chi_0 w_0$, where χ_0 is the parameter controlling the beam that will tend to the Gaussian vortex beam with a larger value and the Airy vortex beam with a smaller value, x_d and y_d are the dislocation of the optical vortex from the x and y axes, respectively. We will deduce the analytic expression of the AiGV beams with $x_d = y_d = 0$ in this section.

The AiGV beams with $l = 1$ can be referred to the first-order AiGV beams and $l = 2$ to the second-order AiGV beams. In the situation of $l = 1$ and $l = 2$, we calculate the initial incident of the AiGV beam intensity and phase with $x_d = y_d = 0$ and $x_d = y_d \neq 0$, respectively. And $x_d = y_d = 0$ means the vortex overlaps the main lobe of the AiGV beams; $x_d = y_d \neq 0$ means the vortex do not overlap the main lobe of the AiGV beams.

Clearly, we find that, in Fig. 1 as the l increases, the vortex further weakens the main lobe of the AiGV beams and further strengthens the sidelobe of the AiGV beams in the same conditions. Because the l increases, we can see the cycle of the AiGV beams in phase with $l = 2$ is the half of $l = 1$. Thus, the cycle of the AiGV beams will be decreased following the l increase. On the other hand, contrasting the case of $x_d = y_d = 0$ with $x_d = y_d \neq 0$, we easily get the fact that the main lobe of AiGV beams is strengthened, and the sidelobe of the AiGV beams is weakened, as the x_d and y_d increase. Because the vortex direction is changed, it no longer overlaps the main lobe. Besides, as shown in the figure of the phase distribution of the AiGV beams with $x_d = y_d \neq 0$, the direction of the vortex of the AiGV beams is changed as the x_d and y_d increase. And

the vortex of the AiGV beams moves to the upper right because of the $x_d = y_d = 0.5$ mm.

Next, we consider the case of the formula derivation to discover the propagation properties of the AiGV beams. The paraxial transmission of the AiGV beams, which is shown by $E_0(x_0, y_0, 0)$ through the gradient-index media, can be performed with the Huygens diffraction integral [15]. It can be expressed as

$$E_1(x, y, z) = \frac{ik}{2\pi B} \iint_{-\infty}^{\infty} E_0(x_0, y_0, 0) \times \exp \left\{ -\frac{ik}{2B} [A(x_0^2 + y_0^2) - 2(x_0 x + y_0 y) + D(x^2 + y^2)] \right\} dx_0 dy_0, \quad (2)$$

where the wavenumber is $k = \frac{2\pi}{\lambda}$ in free space and λ is the wavelength of the incident light.

Based on binomial expansion and Airy integral formula, we can denote the general form that applies to any arbitrary order of the AiGV beams. It can be formulated as

$$E_2(x, y, z) = \frac{i^{m_1+1} k A_0}{2\pi B} \exp \left[-\frac{ikD}{2B} (x^2 + y^2) \right] \times \sum_{m_1=0}^l C_l^{m_1} \sum_{m_2=0}^{l-m_1} C_{l-m_1}^{m_2} \sum_{m_3=0}^{m_1} C_{m_1}^{m_3} \times \left(-\frac{x_d}{w_1} \right)^{m_2} \times \left(-\frac{y_d}{w_2} \right)^{m_3} \frac{\partial^{l-m_1-m_2}}{\partial a_1^{l-m_1-m_2}} (F_1) \frac{\partial^{m_1-m_2}}{\partial a_2^{m_1-m_2}} (F_2), \quad (3)$$

where

$$F_1 = \sqrt{\frac{-\pi}{b}} \exp \left(\frac{-c_1^2}{4b} + \frac{c_1}{w_1^3 b^3} - \frac{1}{96w_1^6 b^3} \right) \times \text{Ai} \left(\frac{1}{16w_1^4 b^2} - \frac{c_1}{2w_1 b} \right), \quad (4)$$

$$F_2 = \sqrt{\frac{-\pi}{b}} \exp \left(\frac{-c_2^2}{4b} + \frac{c_2}{w_2^3 b^3} - \frac{1}{96w_2^6 b^3} \right) \times \text{Ai} \left(\frac{1}{16w_2^4 b^2} - \frac{c_2}{2w_2 b} \right), \quad (5)$$

with $b = \frac{1}{w_0^2} - \frac{ikA}{2B}$, $c_1 = \frac{a_1}{w_1} + \frac{ikx}{B}$, $c_2 = \frac{a_2}{w_2} + \frac{iky}{B}$.

In the condition of $l = 1$ in Eq. (3), we obtain the analytical complex field distribution of the AiGV beams when it propagates at the distance to the z axis, which can be formulated as

$$E_3(x, y, z) = \frac{iA_0 k}{2BG} \exp[H(x, y, z)] (F_3 + F_4 + F_5), \quad (6)$$

where

$$\begin{aligned}
 H(x, y, z) = & -\frac{ikD}{2B}(x^2 + y^2) - \frac{k^2}{4GB^2}(x^2 + y^2) + \frac{ik}{8BG^2} \\
 & \times \left(\frac{x}{w_1^3} + \frac{y}{w_2^3} \right) + \frac{ik}{2BG} \left(\frac{a_1x}{w_1} + \frac{a_2y}{w_2} \right) \\
 & + \frac{1}{96G^3} \left(\frac{1}{w_1^6} + \frac{1}{w_2^6} \right) + \frac{1}{8G^2} \left(\frac{a_1}{w_1^4} + \frac{a_2}{w_2^4} \right) \\
 & + \frac{1}{4G} \left(\frac{a_1^2}{w_1^2} + \frac{a_2^2}{w_2^2} \right), \tag{7}
 \end{aligned}$$

$$\begin{aligned}
 F_3 = & \text{Ai}(f(x))\text{Ai}(g(y)) \left[\left(\frac{ikx}{2BGw_1} + \frac{1}{8G^2w_1^4} - \frac{x_d}{w_1} \right) \right. \\
 & \left. + i \left(\frac{ikx}{2BGw_2} + \frac{1}{8G^2w_2^4} - \frac{y_d}{w_2} \right) \right], \tag{8}
 \end{aligned}$$

$$F_4 = \frac{1}{2Gw_1^2} \text{Ai}(g(x)) [a_1 \text{Ai}(f(x)) + \text{Ai}'(f(x))], \tag{9}$$

$$F_5 = \frac{i}{2Gw_2^2} \text{Ai}(f(x)) [a_2 \text{Ai}(g(x)) + \text{Ai}'(g(x))], \tag{10}$$

with $G = \frac{1}{w_0^2} + \frac{ikA}{2B}$, $f(x) = \frac{ikx}{2BGw_1} + \frac{a_1}{2Gw_1^2} + \frac{1}{16G^2w_1^4}$, $g(y) = \frac{iky}{2BGw_2} + \frac{a_2}{2Gw_2^2} + \frac{1}{16G^2w_2^4}$ and $\text{Ai}'(\cdot)$ denoting the derivative of the Airy function.

Additionally, in order to further study the AiGV beams, we denote $l = 2$ in Eq. (3), which can be formulated as

$$\begin{aligned}
 E_4(x, y, z) = & -\frac{ikA_0}{2Bb} \exp \left[-\frac{ikD}{2B}(x^2 + y^2) \right] \\
 & \times \exp \left(-\frac{c_1^2 + c_2^2}{4b} + \frac{c_1}{8w_1^3b^2} + \frac{c_2}{8w_2^3b^2} - \frac{1}{96w_1^6b^3} - \frac{1}{96w_2^6b^3} \right) \\
 & \times (F_6 + F_7 + F_8), \tag{11}
 \end{aligned}$$

where

$$\begin{aligned}
 F_6 = & \frac{1}{w_1^2} \left[-\frac{1}{2b} \text{Ai} \left(\frac{1}{16w_1^4b^2} - \frac{c_1}{2w_1b} \right) \right. \\
 & + \frac{1}{4} \left(\frac{c_1^2}{b^2} - \frac{c_1}{w_1^3b^3} + \frac{1}{8w_1^6b^4} \right) \text{Ai} \left(\frac{1}{16w_1^4b^2} - \frac{c_1}{2w_1b} \right) \\
 & + \frac{1}{2} \left(-\frac{1}{4w_1^4b^3} + \frac{c_1}{w_1b^2} \right) \text{Ai}'_b \left(\frac{1}{16w_1^4b^2} - \frac{c_1}{2w_1b} \right) \left. \right] \\
 & \times \text{Ai} \left(\frac{1}{16w_2^4b^2} - \frac{c_2}{2w_2b} \right), \tag{12}
 \end{aligned}$$

$$\begin{aligned}
 F_7 = & \frac{2i}{w_1w_2} \left[\left(-\frac{c_1}{2b} + \frac{1}{8w_1^3b^2} \right) \text{Ai} \left(\frac{1}{16w_1^4b^2} - \frac{c_1}{2w_1b} \right) \right. \\
 & + \frac{1}{2w_1b} \text{Ai}'_c \left(\frac{1}{16w_1^4b^2} - \frac{c_1}{2w_1b} \right) \left. \right] \\
 & \times \left[\left(-\frac{c_2}{2b} + \frac{1}{8w_2^3b^2} \right) \text{Ai} \left(\frac{1}{16w_2^4b^2} - \frac{c_2}{2w_2b} \right) \right. \\
 & + \frac{1}{2w_2b} \text{Ai}'_c \left(\frac{1}{16w_2^4b^2} - \frac{c_2}{2w_2b} \right) \left. \right], \tag{13}
 \end{aligned}$$

$$\begin{aligned}
 F_8 = & -\frac{1}{w_2^2} \left[-\frac{1}{2b} \text{Ai} \left(\frac{1}{16w_2^4b^2} - \frac{c_2}{2w_2b} \right) \right. \\
 & + \frac{1}{4} \left(\frac{c_2^2}{b^2} - \frac{c_2}{w_2^3b^3} + \frac{1}{8w_2^6b^4} \right) \text{Ai} \left(\frac{1}{16w_2^4b^2} - \frac{c_2}{2w_2b} \right) \\
 & + \frac{1}{2} \left(-\frac{1}{4w_2^4b^3} + \frac{c_2}{w_2b^2} \right) \text{Ai}'_b \left(\frac{1}{16w_2^4b^2} - \frac{c_2}{2w_2b} \right) \left. \right] \\
 & \times \text{Ai} \left(\frac{1}{16w_1^4b^2} - \frac{c_1}{2w_1b} \right), \tag{14}
 \end{aligned}$$

with $b = \frac{1}{w_0^2} - \frac{ikA}{2B}$, $c_1 = \frac{a_1}{w_1} + \frac{ikx}{B}$, $c_2 = \frac{a_2}{w_2} + \frac{iky}{B}$.

Based on the refractive-index distribution of the gradient form, the gradient-index media includes the radial distribution, the axial distribution, and the spherical distribution [12]. And the radial distribution has been widely applied. The refractive index of the gradient radial distribution can be expressed as

$$n = n_0 \left(1 - \frac{r^2}{2\beta^2} \right), \tag{15}$$

n_0 is the refractive index in media axis, r can be expressed as $r^2 = x^2 + y^2$, and β is the factor of gradient refractive index. We express the optical transfer matrix transfer from $z = 0$ to arbitrary z plane region as [11,16]

$$\begin{pmatrix} A & B \\ C & D \end{pmatrix} = \begin{pmatrix} \cos(\frac{z}{\beta}) & \beta \sin(\frac{z}{\beta}) \\ -\frac{\sin(\frac{z}{\beta})}{\beta} & \cos(\frac{z}{\beta}) \end{pmatrix}, \tag{16}$$

where β represents the coefficient of the gradient refractive index. Finally, we substitute Eq. (16) $ABCD$ matrices into Eqs. (6–10) to obtain the analytic expression of the first-order AiGV beams, which propagates through the gradient-index medium. The ballistic trajectory of the first AiGV beams also consists of the movement locus of the AiG beams and the vortex. The ballistic trajectory of the Airy beam in the x - z plane and the y - z plane can be expressed as

$$\begin{aligned}
 s = & \frac{2a\beta^2 \sin^2(\frac{z}{\beta})}{k^2w_0^2w_1 \cos(\frac{z}{\beta})} - \frac{\left(\frac{1}{w_0^4} - \frac{k^2 \cos^2(\frac{z}{\beta})}{4\beta^2 \sin^2(\frac{z}{\beta})} \right) \beta^2 \sin^2(\frac{z}{\beta})}{4w_1^3 \cos(\frac{z}{\beta}) k^2 \left(\frac{1}{w_0^4} + \frac{k^2 \cos^2(\frac{z}{\beta})}{4\beta^2 \sin^2(\frac{z}{\beta})} \right)}, \\
 & (s = x, y). \tag{17}
 \end{aligned}$$

From Eq. (17), we can find that the transmission distance of the ballistic trajectory shows the periodic variation with $L = 2\pi\beta$. And when

$$z = \frac{(2j+1)L}{4}, \quad (j = 0, 1, 2, \dots), \tag{18}$$

the element of matrix $\cos(\frac{z}{\beta}) = 0$; thus, the solution of the special plane from Eq. (17) is uncertain. The numerical calculation and some results about the property of the AiGV beams and the gradient-index medium will be shown in the next section.

3. NUMERICAL ANALYSIS AND DISCUSSION FOR AIRY-GAUSSIAN VORTEX BEAMS

To explore the propagation properties of the AiGV beams through the gradient-index medium, we perform the light intensity distribution of different positions and showed the ballistic trajectory and the phase distribution when the AiGV

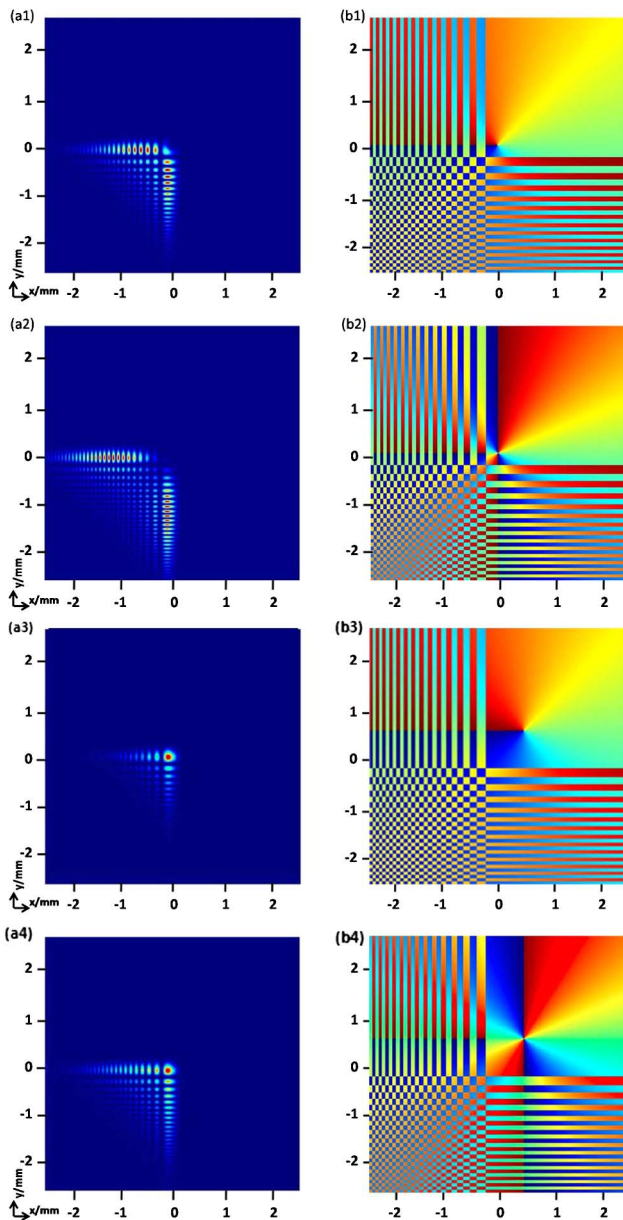


Fig. 1. In the case of $x_d = 0$ and $y_d = 0$, (a1) and (a2) are the intensity of the initial incident AiGV beams with $l = 1$ and $l = 2$, respectively; (b1) and (b2) are the phase distribution of the initial incident AiGV beams with $l = 1$ and $l = 2$. In the case of $x_d = 0.5$ mm and $y_d = 0.5$ mm, (a3) and (a4) are the intensity of the initial incident AiGV beams with $l = 1$ and $l = 2$, respectively; (b3) and (b4) are the phase distribution of the initial incident AiGV beams with $l = 1$ and $l = 2$.

beams are the first- and second-order AiGV beams, respectively. From what has been previously discussed, Eq. (3) is the general analytical expression of the field distribution of the AiGV beams passing through the gradient-index medium. We define that $A_0 = 1$, $\lambda = 623.8$ nm, $a = 0.1$, $A_0 = 1$, $\chi_0 = 0.05$, and $w_1 = w_2 = 0.1$ mm, and the Rayleigh distance is $Z_R = kw_1^2/2 = 4.9646$ cm.

First, we give the propagation process of the first-order AiGV beams in the gradient-index medium in Fig. 2.

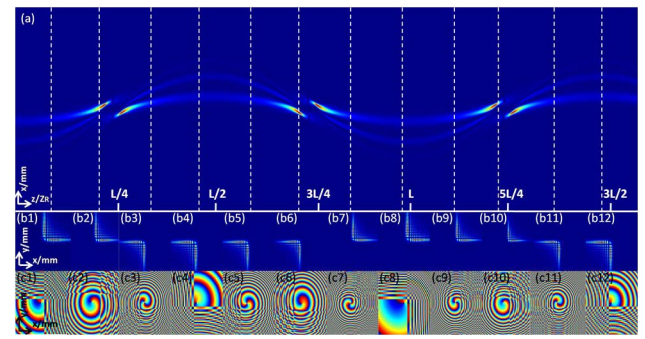


Fig. 2. Numerical demonstration of the first-order AiGV beams propagate through the gradient-index medium. (a) Ballistic trajectory of the first-order AiGV beams in the gradient-index media. (b1)–(b12) Light intensity distributions of the first-order AiGV beams at the different distance in (a). (c1)–(c12) Corresponding phase distributions of the first-order AiGV beams at the different distance in (a). Cut lines indicate the 2D cross section of the light intensity distributions of the first order AiGV beams in the gradient-index media.

Figure 2(a) indicates the ballistic trajectory of the first-order AiGV beams. The bright lines are the track of the first-order AiGV beams. We can see that the propagation path, which has three singularities, is a wavy line performing for a trigonometric function. As the picture shows, in the singularities, the ballistic trajectory is divergent and has spectral anomalies. For example, the ballistic trajectory of the left singularity approaches infinity and appears on the right side approaching negative infinity. The singularities are at the positions of $z = \frac{L}{4}$, $z = \frac{3L}{4}$, and $z = \frac{5L}{4}$, which are corresponding to Eq. (18) with $j = 0$, $j = 1$, and $j = 2$, respectively. Furthermore, the divergent of the track in the singularities is different from the parabola ballistic trajectory in the free space and the uniaxial crystal.

In Fig. 2(b), when it propagates through the direction of the maximum intensity, which is the middle between two singularities with $z = \frac{L}{2}$, the light intensity distribution is symmetric. It can be clearly seen that the beams take the displacement along the 45° axis resulting from its distinctive symmetry. The sidelobe of the light intensity distribution is weakened when closing in on the singularity. As the beams further propagates before the first singularity, the main lobe is reconstructed, and the sidelobe gradually disappears.

At the beginning of the second singularity, the light intensity distribution is a symmetric distribution because of the singularity, and the sidelobe is reconstructed gradually when the beams are close to maximum intensity. These phenomena prove the acceleration and self-healing nature of the first-order AiGV beams.

In addition, Figs. 2(c1)–2(c12) show the corresponding phase distributions. We can see the rotation direction of the vortex changes after the first order AiGV beams propagate through the direction of singularity and the maximum intensity. Besides, the properties of gradient-index medium make the light intensity distribution and the direction of the vortex change oppositely.

To delve into the propagation properties of the second-order AiGV beams, we carry out some numerical calculations and present the phenomenon according to Eqs. (11) and (12).

Similar with the first-order AiGV beams, the ballistic trajectory of the second-order AiGV beams are shown as the trigonometric function distribution. However, because of the second order, the influence of vortex factor is stronger than that of the first-order vortex factor. Owing to the influence of the vortex, the bright line is not clear.

As shown in Figs. 3(b1)–3(b12), the main lobe of the AiGV beams is blocked completely by the vortex and disappears because of the vortex factor.

In addition, Figs. 3(c1)–3(c12) present the phase of the second-order AiGV beams, and it is the half of the phase of the first-order AiGV beams, which is the same as the phase distribution of the initial incident the AiGV beams, as shown in Fig. 2.

Next, in order to investigate the influence of the parameter χ_0 on the ballistic trajectory of the AiGV beams with the first and second orders, we make a numerical simulation to show the influence of the parameter χ_0 and the different between the first- and second-order AiGV beams.

Compared with the first-order AiGV beams in Fig. 4, Fig. 5 indicates that the curve of the fluctuation of the second-order AiGV beams is stronger than the first-order AiGV beams, and the space of the singularity is bigger. Because the amplitude and the vortex factor of the second-order AiGV beams are stronger than that of the first-order. As χ_0 increases, the light intensity distribution of the AiGV beams gradually changes into Gaussian type from Airy type. It can show that the light intensity region is bigger with χ_0 increasing.

In addition, owing to blocking out by the vortex, the propagation trace also is clearer than that with a smaller χ_0 at the same propagation distance and the main lobe disappears.

Last, we explore the beam center of the first- and second-order AiGV beams to observe the ballistic trajectories of the first- and second-order AiGV beams from different angles.

Figure 6 clearly shows the position of the centroid of the AiGV beams on propagation through the gradient-index medium. When the parameter χ_0 is 0.05, the AiGV beams tend

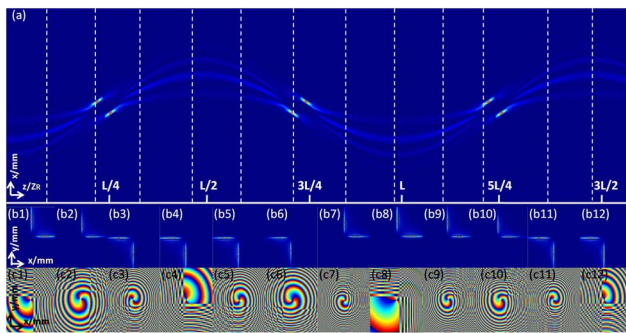


Fig. 3. Numerical demonstration of the second-order AiGV beams propagation through the gradient-index medium. (a) Ballistic trajectory of the second-order AiGV beams in the gradient-index media. (b1)–(b12) Light intensity distributions of the second-order AiGV beams at the different distance in (a). (c1)–(c12) Corresponding phase distributions of the second-order AiGV beams at the different distance in (a). Cut lines indicate the 2D cross section of the light intensity distributions of the second-order AiGV beams in the gradient-index media.

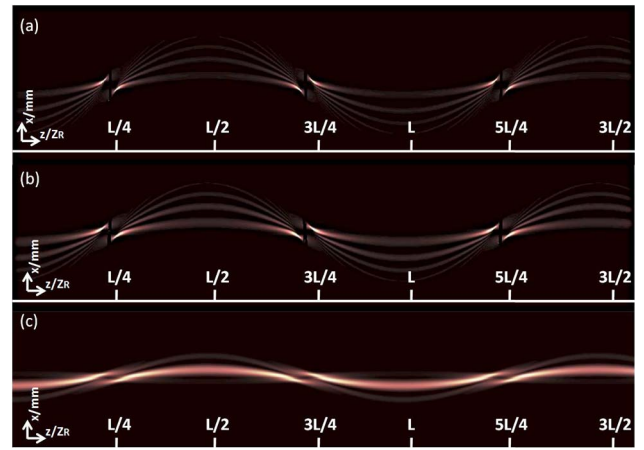


Fig. 4. Numerical demonstrations of ballistic trajectories of the first-order AiGV beams in the gradient-index media. (a)–(c) Numerically simulated the side-view propagation of the first-order AiGV beams with (a) $\chi_0 = 0.05$, (b) $\chi_0 = 0.1$, (c) $\chi_0 = 0.3$.

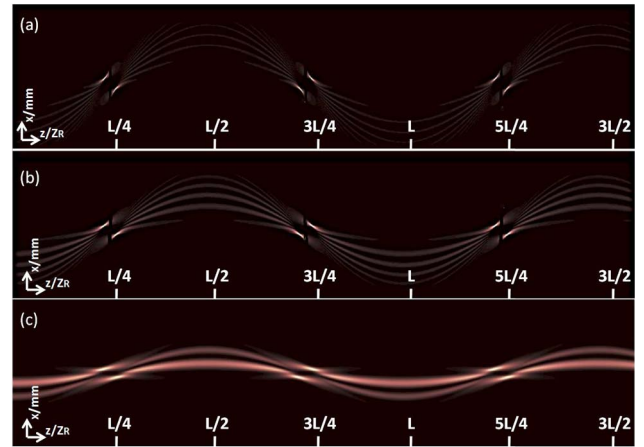


Fig. 5. Numerical demonstrations of the ballistic trajectories of the second-order AiGV beams in the gradient-index media. (a)–(c) Numerically simulated the side-view propagation of the first order AiGV beams with (a) $\chi_0 = 0.05$, (b) $\chi_0 = 0.1$, (c) $\chi_0 = 0.3$.

to be Airy vortex beams. When χ_0 is 0.5, the AiGV beams tend to be Gaussian vortex beams.

Besides, we can find that there are three singularities, which are similar to three breakpoints in the propagation path of the

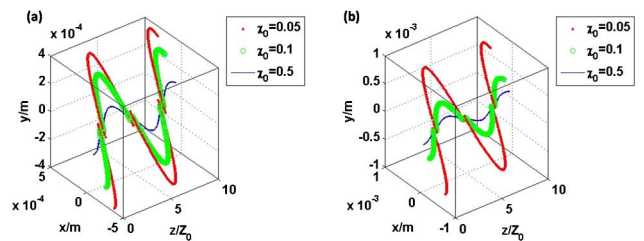


Fig. 6. Numerical demonstrations of the beam center of (a) first-order AiGV beams and (b) second-order AiGV beams propagation through the gradient-index medium.

AiGV beam. When the first- and second-order AiGV beams have the same χ_0 , the curve of the fluctuation of the second-order AiGV beams is stronger than that of the first-order AiGV beams.

4. POYNTING VECTOR OF AIRY-GAUSSIAN VORTEX BEAMS

The Poynting's theorem is the physical quantity described by the energy flow properties of each point in the electromagnetic field. The propagation properties of electromagnetic fields are closely related to their local energy flow. And the Poynting vector is defined as $\vec{S} = \frac{c}{4\pi} \vec{E} \times \vec{B}$ [17], c denotes the speed of light in vacuum, and \vec{E} and \vec{B} are the electric and magnetic fields, respectively. Besides, we can give a vector potential $\vec{A} = \hat{\zeta} E_1(x, y, z) \exp(-ikz)$, where $\hat{\zeta}$ is an arbitrary polarization. In the Lorenz gauge, assuming an \hat{x} -polarized field, the time-averaged Poynting vector can be expressed as [18]

$$\begin{aligned} \langle \vec{S} \rangle &= \frac{c}{4\pi} \langle \vec{E} \times \vec{B} \rangle \\ &= \frac{c}{8\pi} (i\omega(E_1 \nabla_{\perp} E_1^* - E_1^* \nabla_{\perp} E_1) + 2\omega k |E_1|^2 \hat{z}), \end{aligned} \quad (19)$$

where $\nabla_{\perp} = \frac{\partial}{\partial x} \vec{e}_x + \frac{\partial}{\partial y} \vec{e}_y$, \vec{e}_x , \vec{e}_y , and \vec{e}_z are the unit vectors along the x , y , and z directions, respectively, and * denotes the complex conjugate.

In Fig. 7, the coordinate axis, which is on the left bottom, the positive axis; the top right corner is the negative half-axis. Clearly, we can find that the distribution of the energy flow in the z direction is proportional to the light intensity distribution. For observing the changes of the energy flux density of both the first- and second-order AiGV beams, we will perform numerical simulations of the Poynting vector with different propagation distance, which corresponds to Fig. 2 and Fig. 3, respectively.

Figures 7(a1)–7(a12) show the Poynting vector of the first-order AiGV beams with the different propagation distance. It is easy to find that there is a vortex near the origin because of the paraxial approximation. When propagating through the

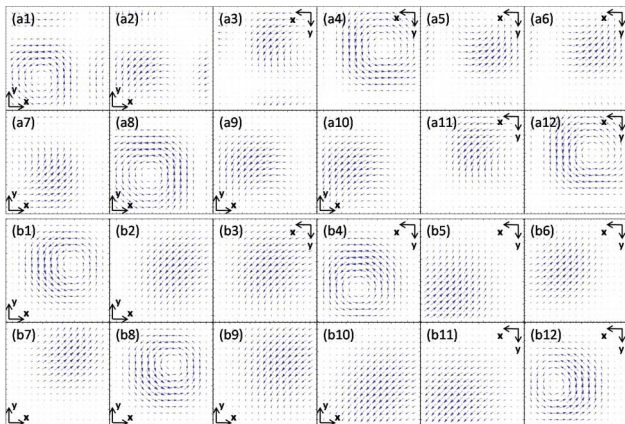


Fig. 7. Numerical demonstrations of the AiGV beams propagating through the gradient-index medium. (a1)–(a12) Poynting vector of the first-order AiGV beams in the same positions as in Fig. 2 with $\chi_0 = 0.1$. (b1)–(b12) Poynting vector of the second-order AiGV beams in the same positions as in Fig. 3 with $\chi_0 = 0.1$.

direction of the maximum intensity, which is the midpoint between two singularities, the vortex is clear, such as in Figs. 7(a1), 7(a4), 7(a8), and 7(a12). The vortex also is weakened gradually as closing the singularity. Besides, the distribution of the vortex is the same as the light intensity distribution, which turns 180° and is inversion symmetry.

On the other hand, Figs. 7(b1)–7(b12) indicate that the Poynting vector of the second-order AiGV beams with the different propagation distance. What is different about the Poynting vector between the first- and second-order AiGV beams is the direction of the vortex because the propagation velocity of the second-order AiGV beams is faster than the first order. This is why the direction of the second-order vortex is far from origin than that of the first order.

5. CONCLUSIONS

In conclusion, we have obtained the analytic expression of the AiGV beams, which propagate through the gradient-index medium. Furthermore, we investigated the propagate path, intensity distributions, phase distributions, and the Poynting vector of the first- and the second-order AiGV beams. Simulation results demonstrate that the AiGV beams have the singularities of the ballistic trajectory divergence propagating in the gradient-index medium at the position of $z = \frac{(2j+1)L}{4}$. Because the accelerated speed tends to infinity and the negative infinity at the specified distance. The gradient-index medium possesses a lens-like effect, which leads to the lobe becoming the negative infinity and no longer meeting the paraxial approximation. This phenomena are different from the parabolic trajectory propagating through free space and the uniaxial crystal. Besides, near the singularity, it is easy to find that the light intensity, the phase distribution, and the Poynting vector are reverse because of the property of the gradient-index medium. In critical distance, the main lobe is shaded by the vortex. As the order increases, we can see clearly that the vortex affects the intensity distribution, the phase distribution, the propagation path, and the Poynting vector of the AiGV beams more from the figure shown above. The cycle of the AiGV beams will be decreased following the l increase. The main lobe is weakened, and the sidelobe is strengthened when the order increases because of the influence of the vortex factor. Besides, the sidelobe and vortex disappear gradually when the AiGV beams propagate closing to the singularity. Additionally, compared with the first-order AiGV beams, the vortex of the second-order AiGV beams is larger and the propagation velocity is faster. Thus, the propagation velocity is raised as the order increases. It has a big influence in the propagation path, the light intensity, the phase distribution, and the Poynting vector of the second-order AiGV beams.

Funding. National Natural Science Foundation of China (NSFC) (11374108, 10904041, 11374107); Foundation of Cultivating Outstanding Young Scholars (Thousand, Hundred, Ten Program) of Guangdong Province in China; Chinese Academy of Sciences (CAS) Key Laboratory of Geospace Environment, University of Science and Technology of China; National Training Program of Innovation and Entrepreneurship for Undergraduates (2015093).

REFERENCES

1. G. A. Siviloglou and D. N. Christodoulides, "Accelerating finite energy Airy beams," *Opt. Lett.* **32**, 979–981 (2007).
2. G. A. Siviloglou, J. Broky, A. Dogariu, and D. N. Christodoulides, "Observation of accelerating Airy beams," *Phys. Rev. Lett.* **99**, 213901 (2007).
3. G. A. Siviloglou, J. Broky, A. Dogariu, and D. N. Christodoulides, "Ballistic dynamics of Airy beams," *Opt. Lett.* **33**, 207–209 (2008).
4. J. Broky, G. A. Siviloglou, A. Dogariu, and D. N. Christodoulides, "Self-healing properties of optical Airy beams," *Opt. Express* **16**, 12880–12891 (2008).
5. J. Baumgartl, M. Mazilu, and K. Dholakia, "Optically mediated particle clearing using Airy wavepackets," *Nat. Photonics* **2**, 675–678 (2008).
6. H. Cheng, W. Zang, and W. Zhou, "Analysis of optical trapping and propulsion of Rayleigh particles using Airy beam," *Opt. Express* **18**, 20384–20394 (2010).
7. Z. Zheng, B. F. Zhang, and H. Chen, "Optical trapping with focused Airy beams," *Appl. Opt.* **50**, 7040–7045 (2011).
8. D. Han, C. Liu, and X. Lai, "The fractional Fourier transform of Airy beams using Lohmann and quadratic optical systems," *Opt. Laser Technol.* **44**, 1463–1467 (2012).
9. B. Chen, C. D. Chen, X. Peng, and D. M. Deng, "Propagation of airy Gaussian vortex beams through slabs of right-handed materials and left-handed materials," *J. Opt. Soc. Am. B* **32**, 173–178 (2015).
10. P. P. Pan, Y. Q. Dan, and B. Zhang, "Propagation of partially coherent flat-topped beams in gradient-index media," *Acta Opt. Sin.* **28**, 1252–1256 (2007).
11. M. A. Bandres and J. C. Gutierrez-vega, "Airy-Gauss beams their transformation by paraxial optical systems," *Opt. Express* **15**, 16719–16728 (2008).
12. H. Y. Song, T. R. Song, S. H. Chen, Y. C. Huang, Y. T. Li, and W. L. Zhang, "Propagation properties of cosine-Gaussian beams in gradient-index medium," *High Power Laser Part. Beams* **23**, 890–894 (2011).
13. H. T. Dai, Y. J. Liu, D. Luo, and X. W. Sun, "Propagation dynamics of an optical vortex imposed on an Airy beam," *Opt. Lett.* **35**, 4075–4077 (2010).
14. O. Livier and M. Soares, *Airy Functions and Applications to Physics* (Imperial College, 1986).
15. A. E. Siegman, *Lasers* (University Science, 1986).
16. J. N. McMullin, "The ABCD matrix in arbitrarily tapered quadratic-index waveguides," *Appl. Opt.* **25**, 2184–2187 (1986).
17. M. Bron and E. Wolf, *Principles of Optics*, 7th ed. (Cambridge University, 1999).
18. L. Allen, M. J. Padgett, and M. Babiker, "The orbital angular momentum of light," *Prog. Opt.* **39**, 291–372 (1999).